International Journal of Nanomedicine

Dovepress
open access to scientific and medical research

Open Access Full Text Article

ORIGINAL RESEARCH

Cationic *Antheraea pernyi* Silk Fibroin-Modified Adenovirus-Mediated ING4 and IL-24 Dual Gene Coexpression Vector Suppresses the Growth of Hepatoma Carcinoma Cells

This article was published in the following Dove Press journal:
International Journal of Nanomedicine

Jing Qu[1]
Weiwei Wang[1]
Yanfei Feng[1]
Longxing Niu[1]
Mingzhong Li[1]
Jicheng Yang[2]
Yufeng Xie[3]

[1]National Engineering Laboratory for Modern Silk, College of Textile and Clothing Engineering, Soochow University, Suzhou 215123, People's Republic of China; [2]Cell and Molecular Biology Institute, College of Medicine, Soochow University, Suzhou 215123, People's Republic of China; [3]Department of Oncology, First Affiliated Hospital of Soochow University, Suzhou 215006, People's Republic of China

Correspondence: Mingzhong Li
National Engineering Laboratory for Modern Silk, College of Textile and Clothing Engineering, Soochow University, No. 199 Ren'ai Road, Suzhou 215123, People's Republic of China
Tel +86-512-6706-1150
Fax +86-512-6724-6786
Email mzli@suda.edu.cn

Yufeng Xie
Department of Oncology, First Affiliated Hospital of Soochow University, No.188 Shizi Road, Suzhou 215006, People's Republic of China
Tel +86-512-6778-0645
Email sdxyf@163.com

Introduction: Cancer gene therapy requires both effective tumor suppressor genes and safe vectors that express target genes efficiently. Inhibitor of growth 4 (ING4) inhibits tumor growth via multiple pathways. Interleukin-24 (IL-24) also has tumor-suppressive activity against a broad spectrum of human cancers. Adenovirus (Ad) vectors exhibit high infection efficiency, but potential toxicity related to high doses of adenovirus has led to careful reconsideration of their use in human clinical trials. *Antheraea pernyi* silk fibroin (ASF) is a cytocompatible and biodegradable natural polymer, and it possesses Arg–Gly–Asp sequences exhibiting a high binding affinity and selectivity for $\alpha_v\beta_3$ and $\alpha_v\beta_5$ integrin receptors, which are overexpressed in tumor vessels and most tumor cells.

Methods: In this study, an Arg-Gly-Asp peptide-modified Ad vector coexpressing ING4 and IL-24 was constructed by homologous recombination of the dual gene coexpression transfer plasmid and RGD-modified pAdEasy-1 adenoviral backbone plasmid. The cationic ASF (CASF) was prepared by modifying ASF with low-molecular-weight PEI. The negatively charged Ad vector was modified with CASF to form a CASF/Ad complex.

Results: Human hepatoma carcinoma SMMC-7721 cells and normal hepatic L-02 cells were infected with the CASF/Ad complex, which showed significantly higher infection efficiency than the naked Ad. The CASF/Ad complex could effectively mediate the expression of the target gene ING4 in SMMC-7721 cells and the secretion of the target gene IL-24 from SMMC-7721 cells, thus inducing apoptosis of hepatoma carcinoma SMMC-7721 cells. The viability of SMMC-7721 and L-02 cells infected with the CASF/Ad complex was further assessed, and it was found that the growth of SMMC-7721 cells was significantly inhibited but that the growth and proliferation of L-02 cells were not affected.

Conclusion: The CASF/Ad complex constructed in this study, showing improved infection efficiency and enhanced suppressive effects on human hepatoma carcinoma SMMC-7721 cells, has the potential to reduce the dose of adenovirus and still maintain high infection efficiency and tumor inhibition.

Keywords: silk fibroin, adenovirus, cationic modification, hepatoma carcinoma

Introduction

Human hepatoma carcinoma is one of the most common causes of cancer-related mortality worldwide.[1] The preferred surgical resection still has a poor prognosis because of the clinicopathological invasion and metastasis characteristics of hepatoma carcinoma.[2] Conventional chemotherapy and radiotherapy are associated with

poor survival rates due to the development of cellular resistance to cancer drugs and the lack of tumor cell targetability.[3,4] Cancer gene therapy represents a new and promising therapeutic modality for various types of cancer. Inhibitor of growth 4 (ING4), an intracellular tumor growth inhibitor, may significantly suppress tumor growth via the induction of cell cycle alterations, apoptosis and the inhibition of tumor angiogenesis.[5,6] Interleukin-24 (IL-24), also known as melanoma differentiation-associated gene-7, is a secreted cytokine and membrane receptor-mediated tumor growth suppressor.[7] IL-24 can suppress growth and induce apoptosis in a wide range of human cancers without apparent cytotoxicity to normal cells.[8,9] Tumor cells often contain multiple genetic abnormalities, which limits the efficacy of a single gene-mediated cancer therapy and presents an obstacle to cancer gene therapy because of the difficulty in finding a pivotal gene closely associated with tumor occurrence and progression. It has been proven in our previous work that adenovirus-mediated ING4 and IL-24 coexpression initiates synergistic tumor growth inhibition and apoptosis very possibly via their coordinate and functional links to p53 which can induce a permanent inhibition of cell growth through blocking cell cycle and activating apoptosis.[10,11] Furthermore, the synergistic antitumor activity elicited by Ad-ING4-IL-24 was closely associated with the cooperative activation of extrinsic and intrinsic apoptotic pathways and reduced proangiogenic factor production of VEGF and IL-8 that are important proangiogenic factors involved in tumor angiogenesis, leading to synergistic inhibition of tumor angiogenesis.[12,13]

An important goal of cancer gene therapy is to develop vectors that can efficiently achieve gene expression and reduce side effects from vectors.[14] Recombinant adenovirus (Ad) has the advantages of high transgene expression efficiency, nonintegration into the host genome, the ability to infect both dividing and nondividing cells and the feasibility of making high-titer stocks.[15,16] Owing to its overwhelming accumulation in the liver after systemic administration, high doses of Ad will inevitably result in severe hepatoxicity.[17] Ad surface modification using a nonviral system to generate hybrid vectors is thus required to reduce the dose and enhance the safety of Ad. Lipid and polymer components of nonviral systems have been employed as an alternative approach to generate improved and more effective Ad vectors. For example, the modification of Ad with polyethylene glycol has been investigated to improve Ad retention time and prevent trapping in the liver[18,19] but results in a loss of infection efficiency because polyethylene glycol blocks specific Ad fiber-cellular receptor interactions.[20] Cationic lipids and polymers, including poly-L-lysine and high-molecular-weight polyethylenimine (PEI), have been tested in Ad-mediated gene delivery systems to enhance the infection efficiency and gene expression in various cancer cell types.[21,22] However, high-molecular-weight PEI induces severe cytotoxicity, significantly limiting its usefulness.[23] *Antheraea pernyi* silk fibroin (ASF) has excellent biocompatibility and is biodegradable,[24,25] and it also contains abundant Arg-Gly-Asp (RGD) tripeptide sequences.[26,27] These sequences are known as receptors of cell integrins, whose levels are significantly upregulated during tumor angiogenesis.[28,29] Furthermore, ASF side chains contain -COOH, -OH and other chemically active groups, which allow for the binding of molecules with $-NH_2$ and -NH groups.[30] This binding was found to be advantageous for the cationic modification of ASF to package plasmid DNA and improve transfection efficiency. Meanwhile, ASF showed significantly lower cytotoxicity than high-molecular-weight PEI in previous studies.[31]

We hypothesized that the positively charged cationic ASF (CASF) modified with low-molecular-weight PEI (1.8 kDa) governed the electrostatic interaction with the negatively charged surface of Ad-mediated ING4 and IL-24 dual gene vector, and the infection efficiency of CASF-coated Ad vector would be greater than the naked Ad. The expression and secretion of the tumor suppressor genes ING4 and IL-24 in CASF/Ad complex were further assessed. The apoptosis of human hepatoma carcinoma SMMC-7721 cells induced by the CASF/Ad complex as well as its cytotoxicity in human normal hepatic L-02 cells were evaluated.

Materials and Methods

Materials

Antheraea pernyi raw silk fibers were purchased from Liaoning Province (China). PEI (MW 1.8 kDa), 2-(N-morpholino)-ethanesulfonic acid, 1-ethyl-3-(3-dimethylaminopropyl) carbodiimide hydrochloride and trypsin were purchased from Sigma-Aldrich (USA). The ultrafiltration centrifuge tube (MWCO 10,000) and 0.22 μm filter were purchased from Millipore (USA). The ethidium bromide (EB), nitrocellulose membrane, bovine serum albumin, horseradish peroxidase-conjugated secondary goat anti-rabbit IgG antibody and Cell Counting Kit-8 (CCK-8) were all purchased from Beyotime (China). The phosphate-buffered saline (PBS) and Dulbecco's modified Eagle medium (DMEM) were both purchased from Gibco (USA). The lysis buffer was purchased from CWBIO (China). The primary rabbit anti-human ING4

antibody was purchased from Abcam (UK). The IL-24 enzyme-linked immunosorbent assay (ELISA) kit was purchased from Westang Bio-Tech (China). The Annexin V/PE and 7-ADD were purchased from BD Biosciences (China). The primers specific to ING4 (ING4-F, 5′-tag aga tct gcc acc atg gct gcg ggg atg tat ttg-3′ and ING4-R, 5′-acc gtc gac cct att tct tct tcc gtt ctt g-3′), IL-24 (IL-24-F, 5′-gca ctc gag acc atg aat ttt caa cag agg ctg ca-3′ and IL-24-R, 5′-gct tct aga tca gag ctt gta gaa ttt ctg-3′) and polyA+promoter (polyA-F, 5′-acc gtc gac aaa cct gcc cca aac aaa tat g-3′ and promoter-R, 5′-gac gcg gcc gct ctc ctc tgt gat atc ctt tc-3′) were synthesized by Shanghai Sangon Biotech co., LTD (China) (Supporting materials). The human embryonic kidney QBI-293A cells were provided by the Department of Oncology, First Affiliated Hospital of Soochow University (China). The human hepatoma carcinoma SMMC-7721 cells and human hepatic L-02 cells were both purchased from the American Type Culture Collection (ATCC, USA). The experiments were formally reviewed and approved by the ethics committee of Soochow University. Reviewed by the ethics committee, the experimental design and implementation have fully considered the principle of security; the experimental content did not exist potential damage and risk and followed the principles outlined in the Declaration of Helsinki.

Preparation of CASF

The ASF solution was prepared as previously described.[31] One hundred grams of *Antheraea pernyi* raw silk fibers were degummed 3 times in 5 L of sodium carbonate (2.5 g/L) and then rinsed thoroughly with deionized water. After drying in an oven at 60 °C, the extracted ASF fibers were dissolved in melted calcium nitrate 4-hydrate at a 1:10 (w/v) bath ratio at 105 °C for 5 h. The ASF solution was obtained after 4 days of dialysis in deionized water at 4 °C.

Next, 30 mL of the ASF solution at a concentration of 1 mg/mL was stirred in an ice bath. PEI was dissolved in tri-distilled water at a concentration of 4 mg/mL and then added to the ASF solution at PEI/ASF weight ratios of 0%, 0.1%, 0.5%, 1%, 2%, 4%, 6% and 8%. After the pH was adjusted to 7.8~8.0 with 0.1 M 2-(N-morpholino)-ethanesulfonic acid solution, 1-ethyl-3-(3-dimethylaminopropyl) carbodiimide hydrochloride accounting for 20% of the ASF quantity was added, and the reactants were slowly stirred overnight in an ice bath. The mixed solution was dialyzed against deionized water at 4 °C for 3 days and then centrifuged three times in an ultrafiltration centrifuge tube for 30 mins to obtain the CASF solution.

Identification of CASF

The zeta potential of the CASF at different PEI/ASF weight ratios was measured by nanoparticle size and zeta potential analyzer (Zetasizer Nano ZS90; Malvern, UK) at 25 °C. Each sample was measured for three times.

Freeze-dried ASF, CASF (modified with 4 wt% PEI against ASF) and liquid PEI (5 mg of each sample) were dissolved in D_2O at room temperature, and the solutions were transferred into a nuclear magnetic tube that used a superconducting nuclear magnetic resonance (NMR) spectrometer (AVANCE III HD 400 MHz; Bruker, USA) to assess the ^{1}H-NMR spectra.

Construction of the Recombinant Ad Vector

The recombinant Ad vector coexpressing ING4 and IL-24 tumor suppressor genes was constructed as described in our previous study.[10] Briefly, the ING4 and IL-24 cDNA fragments were amplified by polymerase chain reaction (PCR) using pAdTrack-CMV-ING4 or pAdTrack-CMV-IL-24 plasmids as templates and primers specific for ING4 or IL-24. The ING4 and IL-24 fragments were then subcloned into the pAdTrack-CMV-polyA+promoter transfer plasmid encoding green fluorescent protein (GFP) gene at Bgl II, Sal I and Xhol I, Xbal I sites, respectively. ING4 transcription was under the control of the cytomegalovirus (CMV) promoter, and IL-24 transcription was under the control of the SV40 polyA+hEF1α-eIF4g promoter (polyA+promoter).

The recombinant Ad vector RGD.Ad-ING4-IL-24 was subsequently generated by homologous recombination of the dual gene coexpression transfer plasmid and RGD-modified pAdEasy-1 adenoviral backbone plasmid (containing most of the genome of human adenovirus type 5) in BJ5183 bacteria and then packaged and amplified in QBI-293A human embryonic kidney cells. The titer of the purified Ad was determined using the gene transfer unit method by calculating the number of GFP reporter gene-expressing QBI-293A cells within 24 h of adenoviral infection by fluorescence microscopy (Olympus, Japan).

Agarose Gel Electrophoresis

The ING4, IL-24 and polyA+promoter cDNA fragments were amplified by PCR using primers specific to ING4, IL-24 and polyA+promoter. The PCR products were loaded onto a 1.0 wt% agarose gel containing EB (0.5 μg/mL) and run in Tris-acetate buffer at 120 V for 40 mins. The electropherogram was obtained by irradiation under ultraviolet light.

Construction and Characteristics of the CASF/Ad Complex

Firstly, 500 μL of the RGD.Ad-ING4-IL-24 with a titer of 2×10^7 pfu/mL and 500 μL of CASF at different concentrations of 10, 50, 100 and 150 μg/mL were mixed, respectively. Then, the mixtures were swirled for 30 s and incubated for 30 mins at room temperature to form the CASF/Ad complexes. The CASF/Ad complexes were then filtered through a 0.22 μm filter to remove the remaining CASF and Ad.

The CASF/Ad complexes were vacuum-dried and sputter-coated with gold, and the surface morphology was observed with scanning electron microscopy (S-4800; Hitachi, Japan).

The average diameters of the naked Ad and the CASF/Ad complexes were analyzed using SEM images with Nano Measurer analysis software (Department of Chemistry, Fudan University, China. Copyright: (C) 2008 Jie Xu). The average equivalent circular diameter was determined by a total of 100 particles.

The zeta potentials of the naked Ad and the CASF/Ad complexes were measured by nanoparticle size and zeta potential analyzer at 25 °C. Each sample was measured for three times.

The nano stability of the CASF/Ad complex was further detected. The changes of the average particle diameter and zeta potential at 0 h, 4 h, 8 h, 12 h, 24 h, 48 h and 72 h after the preparation of the CASF/Ad complex (at CASF concentration of 50 μg/mL) were measured, respectively.

ING4 Gene Expression and IL-24 gene Secretion

QBI-293A cells treated with Ad and PBS or human hepatoma carcinoma SMMC-7721 cells treated with CASF/Ad, Ad and DMEM for 48 h were collected, washed with cold PBS and lysed in lysis buffer (1×10^7 cells/mL lysis buffer). Total cell lysates were resolved by 12% sulfate-polyacrylamide gel electrophoresis and subsequently transferred to a nitrocellulose membrane. The membrane was blocked with 5% (w/v) bovine serum albumin for 1 h at 37 °C, incubated with a primary rabbit anti-human ING4 antibody in the blocking solution for 1 h and then incubated with a horseradish peroxidase-conjugated secondary goat anti-rabbit IgG antibody for an additional hour. Subsequently, the membrane was washed 3 times in TBST, immersed in a chemiluminescence solution and incubated for 3 mins at room temperature. The protein bands were visualized after exposure of the membranes to X-ray film.

QBI-293A cells were treated with Ad and PBS for 24 h and 48 h, or human hepatoma carcinoma SMMC-7721 cells were treated with CASF/Ad, Ad and DMEM for 24 h and 48 h. The cell culture supernatant from each group was harvested. The IL-24 concentration in each group was measured using an ELISA kit.

GFP Expression

The ratio of infectious Ad to target cells is called the multiplicity of infection (MOI) in the present study. To assess the optimal MOI for maximal transgene expression, SMMC-7721 and L-02 cells were infected with the RGD.Ad-ING4-IL-24 at MOIs of 0, 5, 10, 20, 50, 100, 150 and 200, and the GFP expression was examined by laser scanning confocal microscopy (FV1000; Olympus, Japan).

SMMC-7721 and L-02 cells were infected with the naked Ad and the CASF/Ad complex for 24 h, and the GFP expression was examined by laser scanning confocal microscopy.

Infection Efficiency and Cell Apoptosis

The expression level of GFP was determined by flow cytometry analysis. Human hepatoma carcinoma SMMC-7721 cells and human normal hepatic L-02 cells treated with Ad and CASF/Ad complex for 24 h were digested with trypsin, and then the medium containing serum was added to terminate digestion. The cells were washed with PBS and suspended in PBS for the detection of GFP expression by a flow cytometer (FC500; Beckman-Coulter, USA). The number of cells detected per sample was 10,000.

Human hepatoma carcinoma SMMC-7721 cells were treated with CASF/Ad, Ad and DMEM for 48 h, digested with trypsin and then washed twice with PBS. After centrifugation, the cells were suspended in 200 μL of PBS, and the binding buffer was added, maintaining a final cell concentration of 1×10^6 cells/mL. Then, 100 μL of the cell suspension was transferred to a 1.5 mL centrifuge tube, and 5 μL of Annexin V/PE and 10 μL of 7-ADD were added, after which the mixture was incubated in the dark for 15 mins at room temperature. The samples with an extra 400 μL of binding buffer added were assessed by a flow cytometer, and the number of cells detected per sample was 10,000.

Viability of SMMC-7721 and L-02 Cells

Human hepatoma carcinoma SMMC-7721 cells and human normal hepatic L-02 cells were seeded in 96-well culture plates at a density of 1×10^4 cells per well in 100 μL of

growth medium and attached for 24 h. Subsequently, the cells were treated with CASF/Ad, Ad and DMEM for 4 h, the supernatant in each well was removed, and 100 μL of growth medium was added to each well. After culturing for 1, 3, 5 and 7 days, the medium in each well was removed, and 90 μL of DMEM and CCK-8 was added. After incubation for 2 h, the optical density (OD) was measured at 450 nm on a microplate reader (Synergy HT; BioTek, USA), and the cell viability was calculated using the following equation.

$$\text{Cell viability}(\%) = \frac{\text{The OD of experimental group} - \text{The OD of DMEM and CCK-8}}{\text{The OD of blank control group} - \text{TheOD of DMEM and CCK-8}}$$

Statistical Analysis

All data were presented as the means ± standard deviation. The significance of the difference between groups was evaluated by one-way and two-way repeated measures ANOVA and multiple comparisons with SPSS 10.0 software. A value of $p < 0.05$ was considered statistically significant.

Results

Construction and Identification of RGD Ad-ING4-IL-24

The recombinant Ad vector coexpressing ING4 and IL-24 tumor suppressor genes was constructed using our previously described method,[10] and the vector was identified by PCR and agarose gel electrophoresis. Figure 1(A) shows the gel electrophoresis analysis of six extracted clones after homologous recombination of the transfer plasmid and RGD-modified pAdEasy-1 adenoviral backbone plasmid in BJ5183 bacteria. The molecular weights of the 6 selected clones were all larger than that of the transfer plasmid, and were close to that of pAdEasy-1 adenoviral backbone plasmid, indicating that the 6 clones were all positive clones. The ING4, IL-24 and polyA +promoter cDNA fragments of the extracted plasmid were amplified by PCR. Figure 1(B) shows the corresponding gel electrophoretogram, revealing that both the tumor suppressor genes ING4 (750 bp) and IL-24 (621 bp) and the promoter gene polyA+promoter (888 bp) were successfully amplified. In conclusion, a homologous recombinant vector RGD.Ad-ING4-IL-24 was successfully constructed.

The Ad vector-mediated expression of the exogenous target genes ING4 and IL-24 was detected by Western blotting and ELISA. QBI-293A human embryonic kidney cells were treated with the RGD.Ad-ING4-IL-24 for 24 h. Medium containing PBS without adenovirus was used as a control. The Western blotting results in Figure 1(C) showed that the QBI-293A cells infected with the Ad vector produced a 29 kDa anti-ING4 antibody-specific band, while no specific band was observed at the corresponding site for the uninfected cells. Therefore, the exogenous target gene ING4 was successfully expressed from the recombinant Ad vector in QBI-293A cells. QBI-293A cells were treated with the RGD.Ad-ING4-IL-24 for 1 and 2 days to detect the level of secreted IL-24 in the supernatant, and the ELISA results are shown in Figure 1(D). After culture for 1 day, the concentration of IL-24 in the supernatant of QBI-293A cells infected with the Ad vector was 78.1 pg/mL, while the IL-24 concentration in the supernatant of the control cells was 60.1 pg/mL. Two days later, the concentration of IL-24 in the supernatant of the Ad and PBS groups increased to 118.3 and 72.6 pg/mL, respectively. The concentration of IL-24 in the supernatant of the Ad group was significantly higher than that of the PBS group ($p<0.05$), demonstrating that the recombinant Ad vector efficiently mediated the secretion of exogenously expressed IL-24 from QBI-293A cells.

Synthesis and Characteristics of CASF

The -COOH groups in the side chains of the aspartic acid and glutamic acid residues easily lost H^+; thus, the ASF was negatively charged in neutral solution.[32] As shown in Figure 2(A), the carbon-nitrogen double bond (-N=C-) on 1-ethyl-3-(3-dimethylaminopropyl) carbodiimide hydrochloride coupled with the carboxyl groups from the aspartic and glutamic acids in ASF to form an unstable intermediate urea derivative (O-acylisourea). The chemical formula of PEI was $-(CH_2CH_2N(CH_2CH_2NH_2))_n-(CH_2CH_2NH)_{2n}-$, with an abundance of $-NH_2$ groups in the side chains. The O-acylisourea readily reacted with the primary amine groups in PEI, forming an amide linkage between ASF and PEI, and the CASF was synthesized.

Figure 2(B) shows that the zeta potential of ASF was approximately −9.2 mV, which reversed to a positive value after modification using only 0.5 wt% PEI against ASF. The zeta potential continued to increase as the added PEI increased from 1 wt% to 4 wt%, and the zeta potential reached a peak value of +11.4 mV when the mass ratio of PEI/ASF was 4 wt%. Subsequently, as the mass ratio of PEI/ASF increased to 6 wt% and 8 wt%, the zeta potential of CASF decreased slightly, possibly due to the desorption

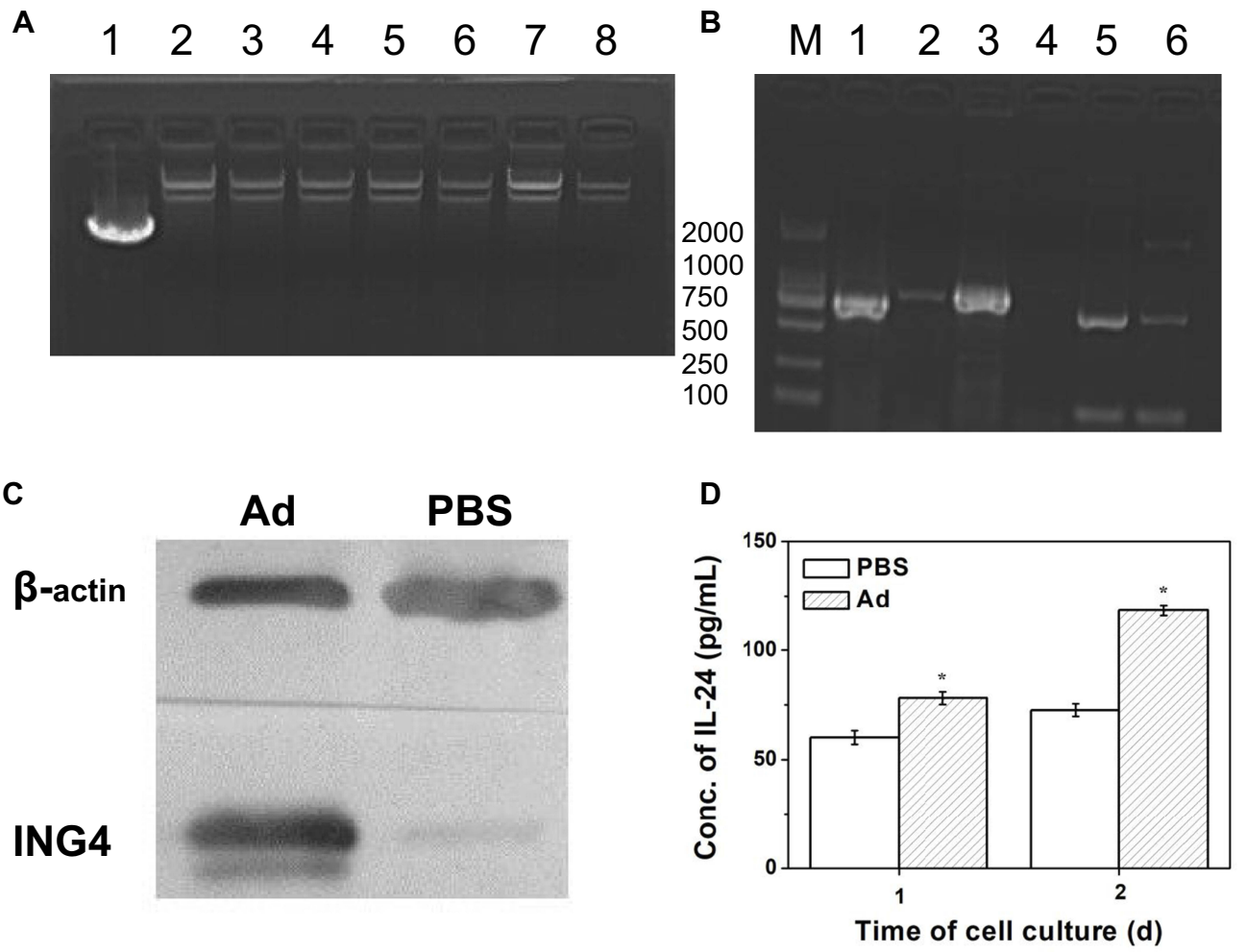

Figure 1 Identification of the RGD.Ad-ING4-IL-24 vector. (**A**) Gel electrophoresis of homologous recombinant adenovirus clones: Line 1, pAdTrack-CMV-ING4-polyA +promoter-IL-24 plasmid; Line 2, pAdEasy-1 adenoviral backbone plasmid; Line 3~8, the 6 selected clones. (**B**) Gel electrophoresis of genes ING4, IL-24 and poly+promoter amplified by PCR: Line 1, ING4 cDNA fragments amplified by PCR; Line 2, negative control group compared to ING4 cDNA fragments amplified by PCR; Line 3, polyA +promoter cDNA fragments amplified by PCR; Line 4, negative control group compared to polyA+promoter cDNA fragments amplified by PCR; Line 5, IL-24 cDNA fragments amplified by PCR; Line 6, negative control group compared to IL-24 cDNA fragments amplified by PCR; M, DL2000 marker. (**C**) The ING4 expression in QBI-293A cells analyzed by Western blotting. (**D**) The IL-24 secretion from QBI-293A cells detected by ELISA. Statistically significant in comparison with PBS, *p<0.05.
Abbreviations: RGD, Arg-Gly-Asp; Ad, adenovirus; ING4, inhibitor of growth 4; IL-24, interleukin-24; CMV, cytomegalovirus; PCR, polymerase chain reaction; ELISA, enzyme-linked immunosorbent assay.

of the partially physically adsorbed PEI. We selected a PEI/ASF ratio of 4 wt% as the optimal cationization ratio for subsequent experiments, which maximized the CASF zeta potential and avoided the introduction of dissociative PEI.

The ^{1}H-NMR spectra of PEI, ASF and CASF are presented in Figure 2(C). The chemical structure of PEI was $-(CH_2CH_2N(CH_2CH_2NH_2))_n-(CH_2CH_2NH)_{2n}-$; thus, the corresponding proton chemical shifts appeared at δ 2.47–2.63 ppm (1, 2, 3 and 4).[33] The chemical shift of 5 (δ, ~1.32 ppm) corresponded to $-CH_2-$, 6 (δ, ~3.06 ppm) to $-C(=O)-N-CH_2-$, 8 (δ, ~3.84 ppm) to -NH- in cystine, and 9 (δ, ~4.11 ppm) to -NH-C(=O)-, all of which appeared on the ASF and CASF spectra.[34,35] In the ^{1}H-NMR spectrum of CASF, a new methylene proton shift corresponding to the amide bond in the $-CONHCH_2CH_2NH-$ structure appeared at 7 (δ, ~3.22 ppm),[36] revealing that a new amide bond was formed by the chemical reaction between the -COOH in ASF and the $-NH_2$ in PEI. The results of the zeta potential and ^{1}H-NMR spectra jointly proved the successful modification of ASF with PEI, which changed the surface charge of ASF from negative to positive.

Cells Infected with Different Titers of Ad

Human hepatoma carcinoma SMMC-7721 cells and hepatic L-02 cells were infected with the RGD.Ad-ING4-IL-24 with a titer of 2×10^{7} pfu/mL at MOIs of 0, 5, 10, 20, 50, 100, 150 and 200. Figure 3 shows the laser confocal fluorescence

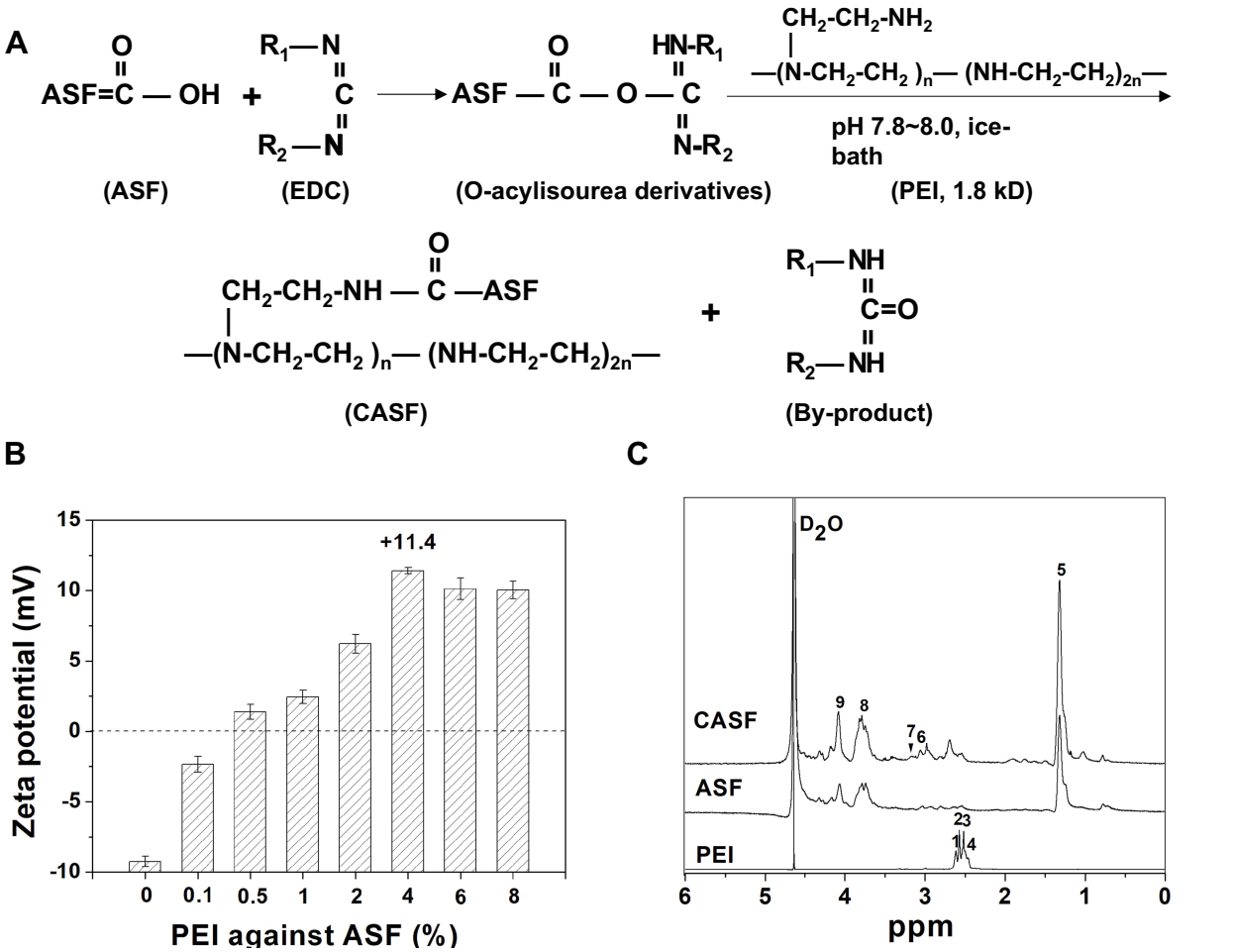

Figure 2 Synthesis and characteristics of CASF. (**A**) Schematic diagram of CASF synthesis. (**B**) Zeta potential of CASF at PEI/ASF weight ratios of 0%, 0.1%, 0.5%, 1%, 2%, 4%, 6% and 8%. (**C**) ^{1}H-NMR spectra of PEI, ASF and CASF in D_2O.
Abbreviations: CASF, cationic *Antheraea pernyi* silk fibroin; PEI, polyethylenimine; ASF, *Antheraea pernyi* silk fibroin; NMR, nuclear magnetic resonance.

images of SMMC-7721 and L-02 cells infected with Ad at different MOIs. As shown in Figure 3(A and C), when the MOI was 0, there was no GFP expression of both SMMC-7721 and L-02 cells; when the MOI increased from 5 to 50, the GFP intensity of both SMMC-7721 and L-02 cells increased gradually. As the MOI increased from 50 to 200, the GFP intensity continued to increase, while its amplitude decreased and tended to be stable, indicating that the higher the Ad titer used for infection was, the higher the fluorescence expression intensity of SMMC-7721 and L-02 cells would be. As shown in Figure 3(B), when the MOI increased from 0 to 50, the SMMC-7721 cells adhered tightly to the culture plate with pseudopodia stretching; as the MOI increased to 100, 150 and 200, the cells became round, and a small number of cells began to float. These results implied that the higher the Ad dose was used, the more obvious the inhibitory effect on hepatoma carcinoma SMMC-7721 cells became. As shown in Figure 3(D), as the MOI increased from 0 to 200, the L-02 cells cultured with Ad adhered tightly to the culture plate at all times, and the cell morphology was not significantly affected. To avoid the potential cytotoxicity caused by high MOI, the MOI of 50 was selected for subsequent experiments.

Stability and Characteristics of the CASF/Ad Complex

The RGD.Ad-ING4-IL-24 was added to CASF solution at CASF concentrations of 10, 50, 100 and 150 μg/mL, and then the mixtures were swirled and incubated for the formation of CASF/Ad complexes. The schematic diagram of the construction of the CASF/Ad complex and the stability of this CASF/Ad system is shown in Figure 4. Figure 4(A) shows that negatively charged Ad was packaged by positively charged CASF with abundant amino groups in the side chains via electrostatic interaction to

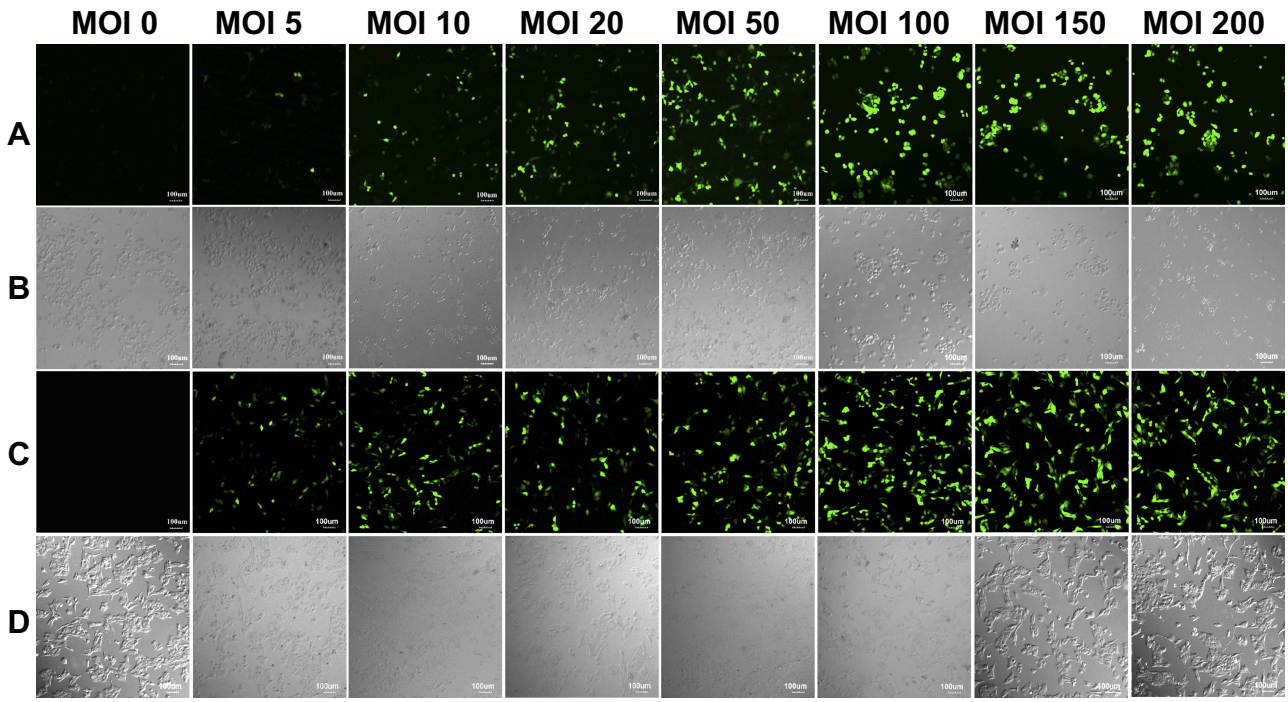

Figure 3 The laser confocal fluorescence images of SMMC-7721 and L-02 cells infected with Ad at MOIs of 0, 5, 10, 20, 50, 100, 150 and 200, respectively. (**A**) Fluorescence field and (**B**) bright-field images of SMMC-7721 cells; (**C**) fluorescence field and (**D**) bright-field images of L-02 cells. Scale bar: 100 μm.
Abbreviations: Ad, adenovirus; MOI, multiplicity of infection.

form CASF/Ad complex. In order to detect the stability of the CASF/Ad complex, the changes of the average particle diameter and zeta potential at 0 h, 4 h, 8 h, 12 h, 24 h, 48 h and 72 h after the preparation of the CASF/Ad complex were measured, respectively. Figure 4(B and C) showed that with the extension of time, the CASF/Ad complex remained round or nearly circular in shape, and the particle diameter increased slightly, but the change was not significant. Figure 4(D) reveals that in the whole process, the zeta potential of the CASF/Ad complex remained stable and decreased slightly but not significantly. These indicated that the shape, particle diameter and zeta potential of the CASF/Ad complex system remained basically stable within 72 h after completion of its preparation.

The scanning electron microscopy images, particle diameter and zeta potential of the CASF/Ad complex formed by coating Ad with CASF at concentrations of 10, 50, 100 and 150 μg/mL are shown in Figure 5. Figure 5(A) shows that both the naked Ad particles and the CASF/Ad complex were sphere-shaped, and the particle diameter of the CASF/Ad complex was larger than that of the naked Ad particle. Figure 5(B and C) showed that the average diameter of Ad was approximately 81.03 nm, and its zeta potential was −9.53 mV. As the concentration of CASF used to coat Ad increased from 10 to 150 μg/mL, the diameter of the CASF/Ad complex accordingly increased from ~128.85 to ~176.75 nm, while the zeta potential increased from ~-8.63 to ~-1.70 mV. The change in zeta potential showed that the negative charge on the surface of the Ad vector was reduced after the CASF coating.

Cells Infected with CASF/Ad Complex

Human hepatoma carcinoma SMMC-7721 cells and human normal hepatic L-02 cells were infected with the naked Ad and the CASF/Ad complex, and the blank control group was the cells cultured in DMEM containing serum. The confocal laser scanning microscopy images of SMMC-7721 and L-02 cells are shown in Figure 6. Figure 6(A and B) show the fluorescence field and bright field images of SMMC-7721 cells, respectively. Figure 6(A) shows that there was no GFP expression in the blank group. As the concentration of CASF used to coat Ad increased from 10 to 50 μg/mL, the green fluorescence intensity of SMMC-7721 cells infected with the CASF/Ad complex obviously increased; when the CASF concentration further increased to 100 and 150 μg/mL, the fluorescence intensity decreased slightly. The GFP intensity of SMMC-7721 cells infected with the CASF/Ad complex was stronger than that of cells infected with the naked Ad. As shown in Figure 6(B), as the concentration of CASF used to coat Ad was 10 μg/mL, the cell morphology of the CASF/Ad group showed no significant

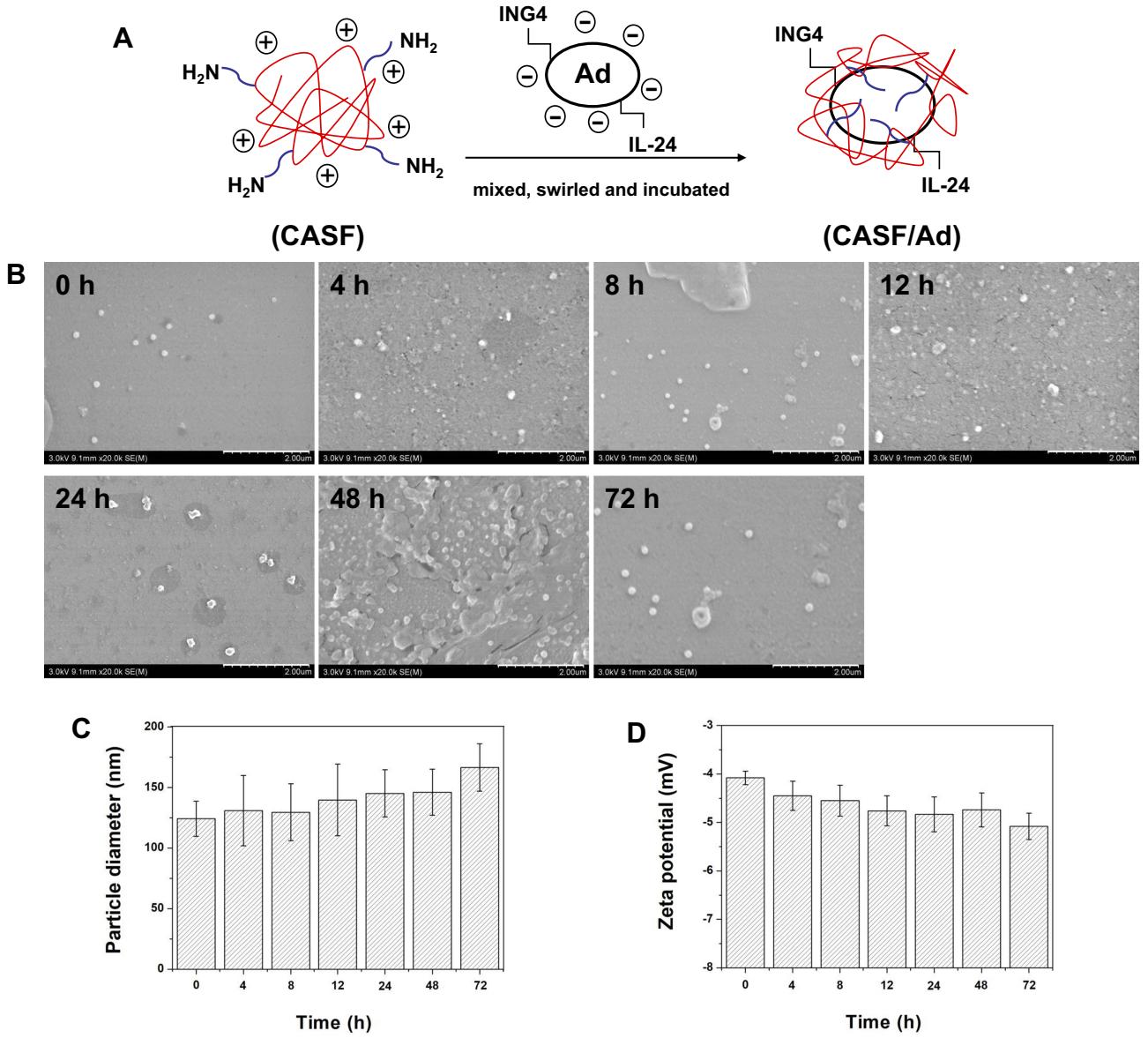

Figure 4 Preparation schematic diagram and stability of the CASF/Ad complex. (**A**) Schematic diagram of the preparation of CASF/Ad complex. (**B**) Scanning electron microscopy images, (**C**) particle diameter and (**D**) zeta potential of the CASF/Ad complex formed by coating Ad with CASF at a concentration of 50 μg/mL at 0 h, 4 h, 8 h, 12 h, 24 h, 48 h and 72 h after the preparation. Scale bar: 2.00 μm.

Abbreviations: CASF, cationic *Antheraea pernyi* silk fibroin; Ad, adenovirus.

difference compared to the blank control group and the Ad group. As the CASF concentration increased to 50, 100 and 150 μg/mL, cells became rounded in shape and gathered into clusters, indicating that cell growth was inhibited and that some cells were dead. Figure 6(C and D) show the fluorescence field and bright field images of L-02 cells, respectively. Figure 6(C) shows that there was no GFP expression in the blank group. When the concentration of CASF used to coat Ad was 10 μg/mL, the green fluorescence intensity of L-02 cells infected with the CASF/Ad complex was similar to that of cells infected with the naked Ad. As the CASF concentration increased to 50 μg/mL, the GFP intensity obviously increased; however, as the concentration of the added CASF further increased to 100 and 150 μg/mL, the GFP intensity tended to decrease. As shown in Figure 6(D), L-02 cells were tightly adhered to the culture plate in both the blank group and the Ad group. When the concentration of CASF used to coat Ad increased from 10 to 150 μg/mL, the cells remained tightly adherent and fully extended into spindle or polygonal shapes. The cells were fully connected to each other, and there were few round dead cells.

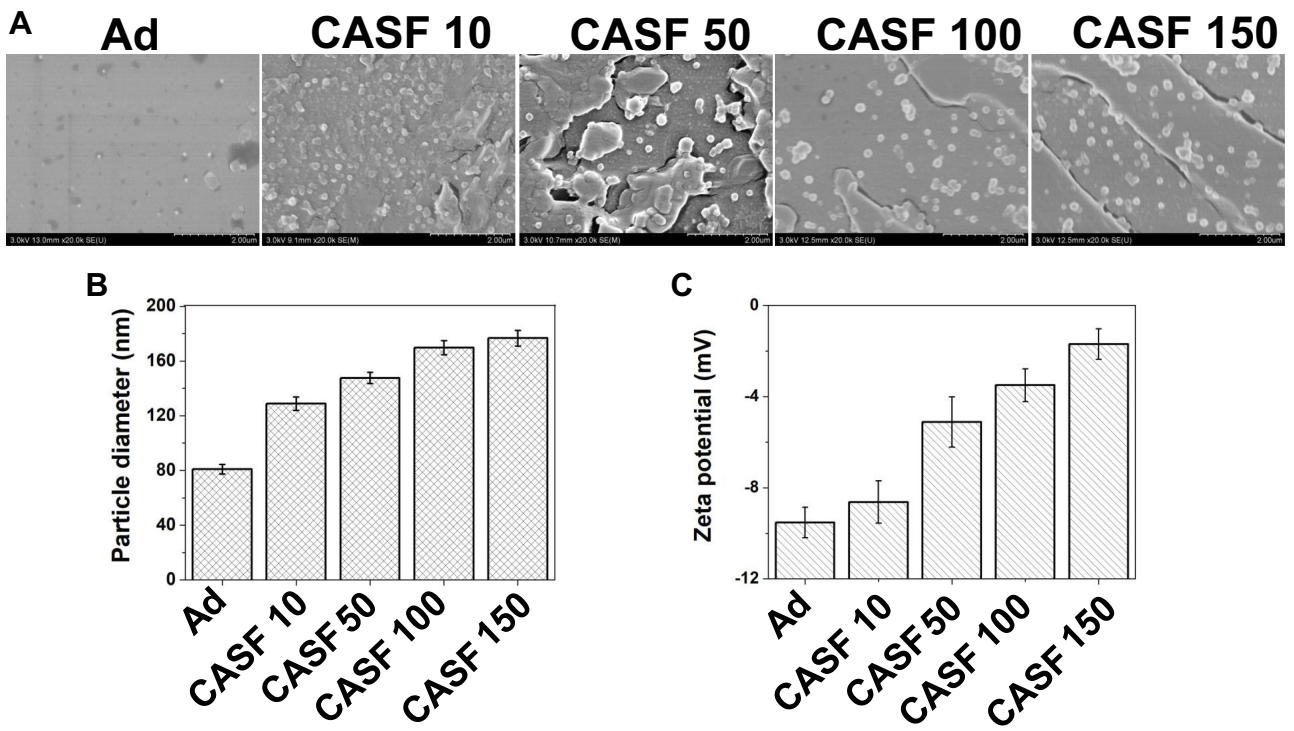

Figure 5 Characteristics of the CASF/Ad complex. (**A**) Scanning electron microscopy images, (**B**) particle diameter and (**C**) zeta potential of the Ad and the CASF/Ad complex. Scale bar: 2.00 μm. CASF 10 to CASF 150 represented the CASF/Ad complexes were formed by coating Ad with CASF at concentrations of 10, 50, 100 and 150 μg/mL, respectively.

Abbreviations: CASF, cationic *Antheraea pernyi* silk fibroin; Ad, adenovirus.

After the SMMC-7721 and L-02 cells were infected with the naked Ad and the CASF/Ad complex, the GFP-positive cells were analyzed by flow cytometry to obtain the infection efficiency. Figure 7 shows the flow cytometry images and infection efficiency of SMMC-7721 and L-02 cells. Figure 7(A) shows that the infection efficiency of SMMC-7721 cells infected with the naked Ad was 60.64%. When the concentration of CASF used to coat Ad increased from 10 to 100 μg/mL, the infection efficiency of SMMC-7721 cells infected with the CASF/Ad complex increased from 83.78% to 92.53%, and when the CASF concentration reached 150 μg/mL, the infection efficiency decreased slightly to 88.06%. Figure 7(B) shows that the infection efficiency of L-02 cells infected with the naked Ad was 65.19%. When the concentration of CASF used to coat Ad increased from 10 to 50 μg/mL, the infection efficiency of L-02 cells infected with the CASF/Ad complex increased from 81.28% to 92.68%, and when the CASF concentration reached 100 and 150 μg/mL, the infection efficiency decreased slightly to 88.76% and 87.73%, respectively. This trend was essentially consistent with the GFP expression pattern observed by laser scanning confocal microscopy. Figure 7(C and D) revealed that the infection efficiency of both SMMC-7721 and L-02 cells infected with the CASF/Ad complex was significantly higher than that of cells infected with the naked Ad ($p<0.01$).

Target Gene Expression from CASF/Ad Complex and Apoptosis of Infected SMMC-7721 Cells

A Western blotting assay was used to assess the expression of the target gene ING4 from the CASF/Ad complex in SMMC-7721 cells, and an ELISA kit was used to detect the secretion level of the target gene IL-24 from the CASF/Ad complex in the cell culture supernatant of SMMC-7721 cells. The results are shown in Figure 8(A and B). As shown in Figure 8(A), SMMC-7721 cells infected with both the CASF/Ad complex and the naked Ad produced 29 kDa anti-ING4 antibody-specific bands, indicating that the RGD.Ad-ING4-IL-24 vector could mediate exogenous ING4 gene expression in SMMC-7721 cells, and the coated CASF did not significantly inhibit exogenous ING4 gene expression. The supernatants of SMMC-7721 cells in the blank control group, Ad group and CASF/Ad complex group were collected, and the

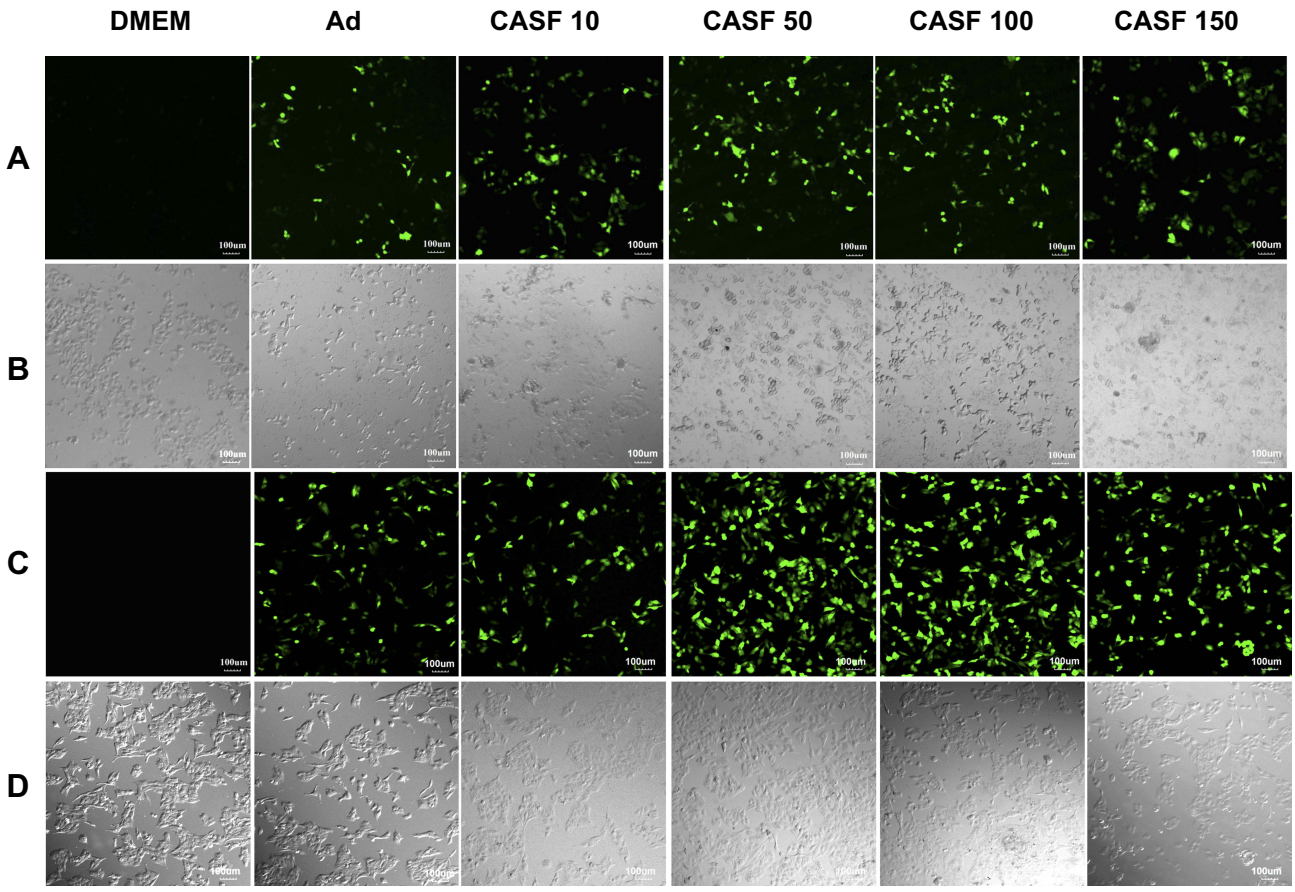

Figure 6 The laser confocal fluorescence images of SMMC-7721 and L-02 cells cultured with DMEM, Ad and CASF/Ad complex for 24 h. (**A**) Fluorescence field and (**B**) bright-field images of SMMC-7721 cells; (**C**) fluorescence field and (**D**) bright-field images of L-02 cells. Scale bar: 100 μm. CASF 10 to CASF 150 represented cells were infected with the CASF/Ad complexes formed by coating Ad with CASF at concentrations of 10, 50, 100 and 150 μg/mL, respectively.
Abbreviations: DMEM, Dulbecco's modified Eagle medium; CASF, cationic *Antheraea pernyi* silk fibroin; Ad, adenovirus.

IL-24 concentration was detected. Figure 8(B) shows that after 1 day of culture, the concentration of secreted IL-24 in the blank control group, Ad group and CASF/Ad group was 55.4, 74.3 and 80.7 pg/mL, respectively, indicating that the secreted IL-24 concentration of both the Ad and CASF/Ad groups was significantly higher than that of the blank control group ($p<0.05$). After 2 days of culture, the expression and secretion of IL-24 from SMMC-7721 cells of the CASF/Ad group increased rapidly, and its concentration reached 110.8 pg/mL, which was significantly higher than that of the Ad group and the blank control group ($p<0.01$), indicating that CASF did not affect the secretion of the exogenously expressed gene IL-24. Furthermore, the level of secreted IL-24 from SMMC-7721 cells infected with the CASF/Ad complex was clearly higher than that from cells infected with the naked Ad at the same dose.

The apoptosis rate of SMMC-7721 cells infected with the CASF/Ad complex was analyzed by flow cytometry, and the results are shown in Figure 8(C and D). Figure 8(C) shows that the apoptosis rates of SMMC-7721 cells cultured with DMEM, Ad and CASF/Ad were 4.65%, 10.86% and 19.20%, respectively. Figure 8(D) shows that the apoptosis rate of SMMC-7721 cells in the CASF/Ad group was significantly higher than that of cells in the Ad and DMEM groups ($p<0.01$).

Proliferation of SMMC-7721 and L-02 Cells

To assess the inhibitory effect of the CASF/Ad complex on hepatoma carcinoma SMMC-7721 cells and its toxicity to hepatic L-02 cells, a CCK-8 assay was used to evaluate cell proliferation. SMMC-7721 and L-02 cells were cultured with DMEM, Ad and CASF/Ad for 1, 3, 5 and 7 days, and the OD of each well was measured to calculate cell viability. The results of cell proliferation are presented in Figure 9. Figure 9(A) shows that the SMMC-7721 cell viability of the DMEM group was essentially maintained at 100% throughout the culture time course. However, the

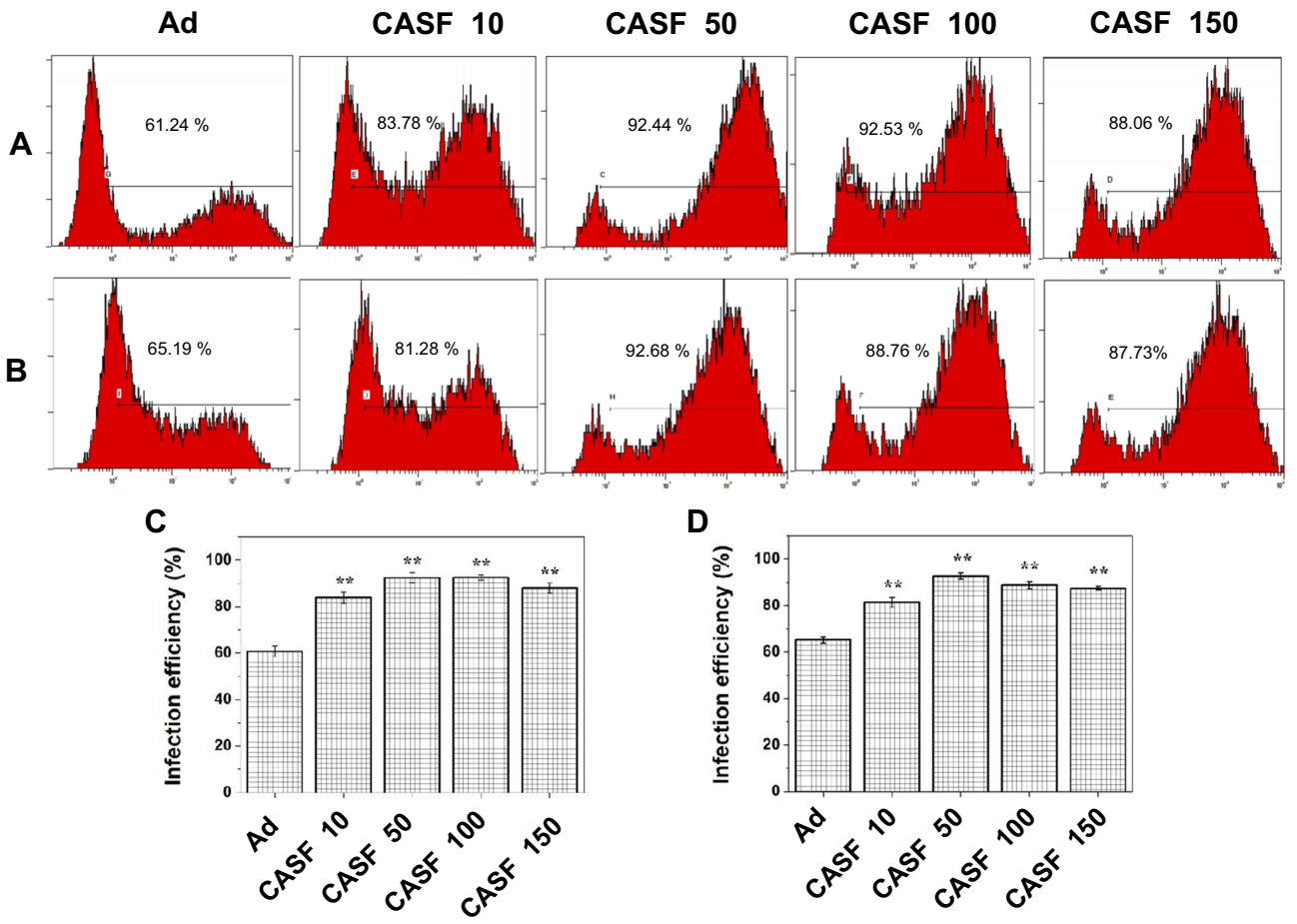

Figure 7 The infection efficiency of cells infected with Ad and CASF/Ad complex for 24 h. The flow cytometry images of (**A**) SMMC-7721 and (**B**) L-02 cells, and the corresponding histogram of infection efficiency of (**C**) SMMC-7721 and (**D**) L-02 cells. CASF 10 to CASF 150 represented cells were infected with the CASF/Ad complexes formed by coating Ad with CASF at concentrations of 10, 50, 100 and 150 μg/mL, respectively. Statistically significant in comparison with naked Ad, **p<0.01.
Abbreviations: CASF, cationic *Antheraea pernyi* silk fibroin; Ad, adenovirus.

cell viability of the Ad group and CASF/Ad group was significantly lower than that of the blank control group (p<0.05). Furthermore, the viability of SMMC-7721 cells infected with the CASF/Ad complex and cultured for 1, 3, 5, and 7 days was 67%, 73%, 75% and 80%, respectively, which was significantly lower than the viability of cells infected with the naked Ad (p<0.05). Figure 9(B) shows that the viability of L-02 cells infected with the CASF/Ad complex and cultured for 1, 3, 5, and 7 days was 88%, 90%, 93% and 90%, respectively, indicating no obvious difference in the viability of cells infected with Ad and cultured with DMEM at the same time points. These results suggested that the ING4 and IL-24 genes expressed from the naked Ad or CASF/Ad complex effectively induced apoptosis of human hepatoma carcinoma SMMC-7721 cells but exhibited no significant inhibitory effect on L-02 normal hepatocytes. In addition, the CASF/Ad complex showed no obvious cytotoxicity in hepatic L-02 cells.

Discussion

Cancer gene therapy has attracted increasing attention in the past few years. ING4 was identified as a potent tumor suppressor gene and has been proven to be involved in carcinogenesis as well as tumor cell proliferation, migration and invasion.[37] Ectopic expression of IL-24 induces growth arrest and apoptosis in malignant human cells but causes minimal lethality toward normal cells.[38] Efficient gene therapy requires the protection of genetic material from degradation and the efficient release from the delivery vector in the tissue and cells of interest.[17] Adenovirus is an excellent candidate for gene delivery because its viral genome is protected by the capsid and is delivered efficiently into coxsackie-adenovirus receptor-positive cells to achieve

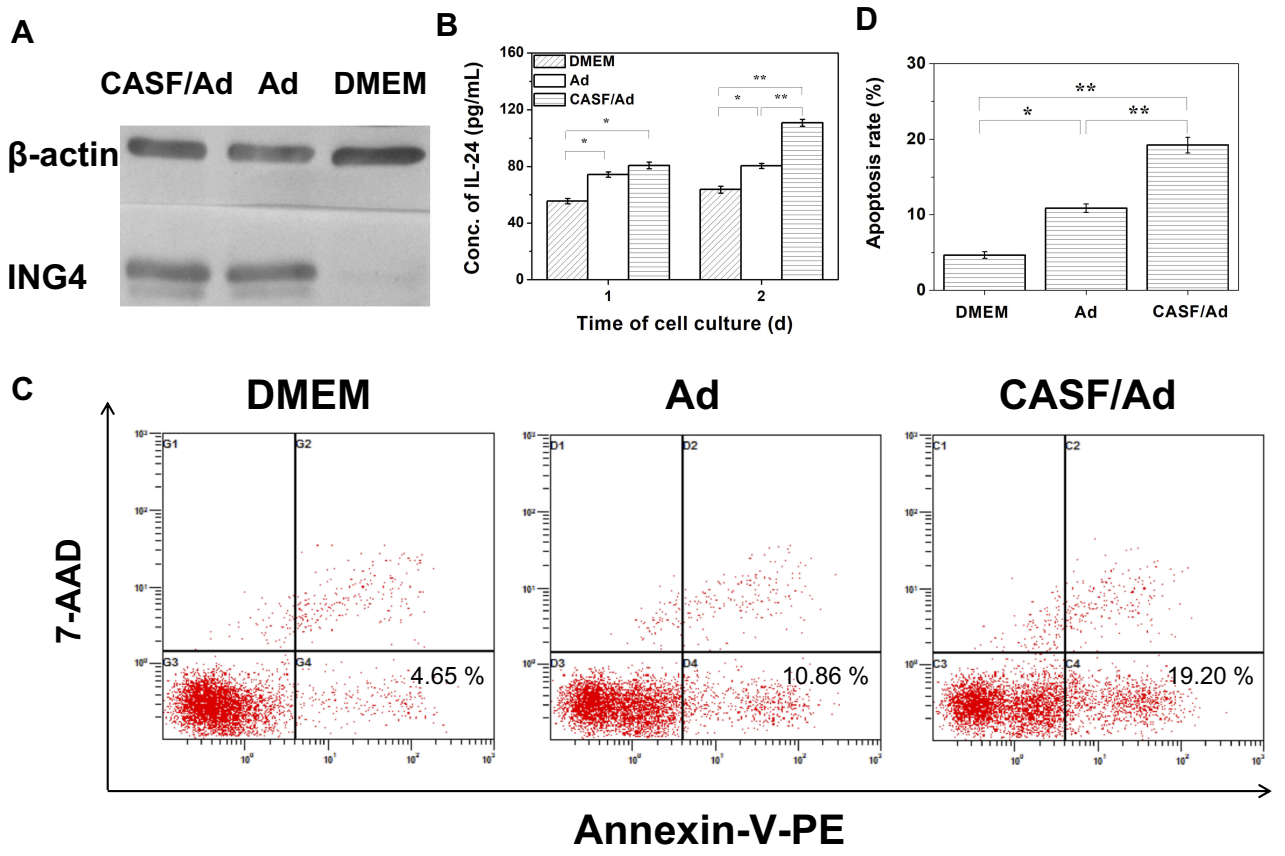

Figure 8 Target gene expression and cell apoptosis. SMMC-7721 cells were cultured with DMEM, Ad and CASF/Ad complex for 48 h. (**A**) The ING4 expression in SMMC-7721 cells analyzed by Western blotting. (**B**) The IL-24 secretion from SMMC-7721 cells detected by ELISA. (**C**) The flow cytometry images and (**D**) the corresponding histogram of apoptosis rates of SMMC-7721 cells. Statistically significant in comparison of CASF/Ad with Ad, DMEM and Ad with DMEM, *p<0.05, **p<0.01.

Abbreviations: DMEM, Dulbecco's modified Eagle medium; Ad, adenovirus; CASF, cationic *Antheraea pernyi* silk fibroin; ING4, inhibitor of growth 4; IL-24, interleukin-24; ELISA, enzyme-linked immunosorbent assay.

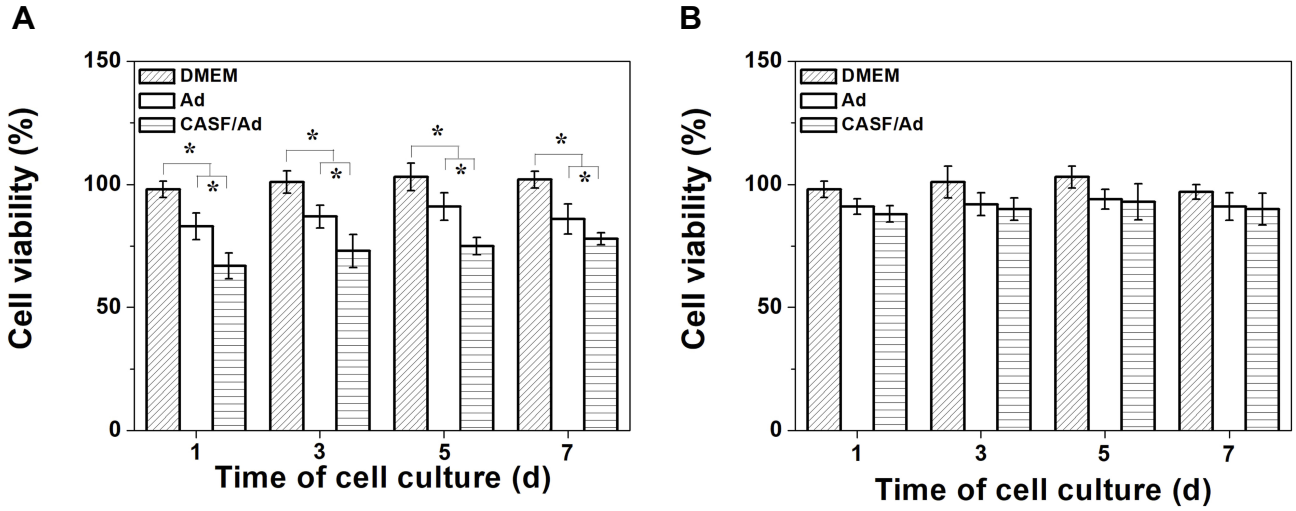

Figure 9 Proliferation of SMMC-7721 and L-02 cells. The cell viability of (**A**) SMMC-7721 and (**B**) L-02 cells cultured with DMEM, Ad and CASF/Ad complex for 1, 3, 5 and 7 days. Statistically significant in comparison of CASF/Ad with Ad, DMEM and Ad with DMEM, *p<0.05.

Abbreviations: DMEM, Dulbecco's modified Eagle medium; Ad, adenovirus; CASF, cationic *Antheraea pernyi* silk fibroin.

high levels of gene expression.[39] In the present study, an RGD-modified Ad vector harboring ING4 and IL-24 tumor suppressor genes was constructed and the expression of the exogenous ING4 and IL-24 genes was further detected. The results suggested that the recombinant Ad vector efficiently mediated ING4 target gene expression in QBI-293A cells and IL-24 gene secretion from QBI-293A cells.

Despite the numerous advantages of Ad vector for cancer gene therapy, the use of high doses of adenovirus inevitably leads to Ad accumulation in the liver and concomitant hepatotoxicity.[15] Modification of Ad to improve its infection efficiency could reduce the dose of Ad used. In this study, ASF was modified with low-molecular-weight PEI containing a large number of amino groups. The zeta potential of CASF reversed to +11.4 mV when the mass ratio of PEI/ASF reached 4 wt%, and the ^{1}H-NMR spectra showed that PEI was successfully bound to ASF macromolecules. Subsequently, CASF was mixed with the RGD.Ad-ING4-IL-24 to prepare the CASF/Ad complex. The RGD.Ad-ING4-IL-24 vector was negatively charged in a neutral environment; as the concentration of the coated CASF increased, the zeta potential of the CASF/Ad complex also increased but remained negatively charged. Cell plasma membranes and Ad are both negatively charged; positively charged polymers are ionically attracted to Ad, and the greatly reduced charge on the Ad surface facilitates viral entry into host cells via electrostatic interactions.[40] Therefore, Ad encapsulation with cationic ASF might be an effective strategy to improve its infection efficiency on cells. The diameter of the naked Ad was approximately 81.03 nm, while the diameter of the CASF/Ad complex concurrently increased with the coating of CASF at an increasing concentration. The major mechanisms of the uptake of nanosized particles by cells are phagocytosis, diffusion, and fluid-phase endocytosis.[41,42] Previous studies have shown that vectors with diameters <200 nm could be effectively accumulated in tumor tissues by enhancing permeability and retention.[43,44] The diameters of the CASF/Ad complexes formed by coating Ad with CASF at concentrations of 10, 50, 100 and 150 μg/mL were 128.85 nm, 147.68 nm, 169.78 nm and 176.75 nm, all of which were below 200 nm; thus, these CASF/Ad complexes were suitable for use as gene vectors to infect cancer cells.

Human hepatoma carcinoma SMMC-7721 cells and normal hepatic L-02 cells were infected with the CASF/Ad complex to study the infection efficiency of the ING4 and IL-24 dual gene coexpression vector. The GFP expression intensity of both SMMC-7721 and L-02 cells infected with the CASF/Ad complex was obviously stronger than that of cells infected with the naked Ad, and as the concentration of CASF used in coating Ad increased, the GFP fluorescence intensity in the infected cells also increased. This was because the combination of CASF with the Ad vector reduced the negative charge on the surface of the Ad vector; consequently, the repulsion between the Ad and the cell surface weakened which increased the access of the CASF/Ad complex to the cell membrane and enhanced its entry into the cells. Comparison of SMMC-7721 with L-02 cells showed that the GFP expression intensity of L-02 cells was obviously stronger than that of SMMC-7721 cells, primarily because the infected SMMC-7721 cell growth was inhibited according to the round shape of the cells and their floating in the medium while the infected L-02 cells were barely affected in terms of the pseudopodia stretching and enhanced adherence to the culture plate. The results of the flow cytometry assay showed that the infection efficiency of the CASF/Ad complex in both hepatoma carcinoma SMMC-7721 cells and hepatocytes was significantly higher than that of the naked Ad, which was consistent with the GFP expression intensity result, further demonstrating that coating the Ad vector with CASF obviously improved its infection efficiency. Ad vectors efficiently transfer genes into cells via the coxsackie-adenovirus receptor and integrins ($\alpha_v\beta3$ and $\alpha_v\beta5$),[45] and the RGD tripeptide sequence can aid the efficient transport of Ad into cells following its interaction with integrins.[46,47] Therefore, compared with the naked Ad, the constructed CASF/Ad complex rich in RGD peptides showed significantly enhanced infection efficiency in the present study.

The CASF/Ad complex could effectively mediate exogenous ING4 gene expression in SMMC-7721 cells and IL-24 gene secretion from SMMC-7721 cells, and the coexpressed ING4 and IL-24 genes acted synergistically on hepatoma carcinoma SMMC-7721 cells, both intracellularly and extracellularly, inducing the apoptosis of tumor cells. The apoptosis rate of SMMC-7721 cells (~19.20%) induced by the CASF/Ad complex was significantly higher than that of cells induced by the naked Ad (~10.86%) and was also slightly higher than the reported apoptosis rate of SMMC-7721 cells induced by adenoviral-mediated p53 gene (~17.8%).[48] The CASF modification and packaging for the RGD.Ad-ING4-IL-24 vector effectively shielded the negative charge on its surface and improved the infection efficiency, leading to the increased expression of the target genes ING4 and IL-24. The RGD peptide, rich in the CASF/Ad complex, has also been shown to induce

apoptosis in tumor cells by blocking the adhesion of tumor cells to the extracellular matrix.[49] The combined effects brought about the enhancement of hepatoma cell apoptosis induced by the CASF/Ad complex.

The nonspecificity of the ING4 and IL-24 dual gene coexpression vector for tumor cells caused high infection efficiency in both hepatoma carcinoma SMMC-7721 cells and normal hepatocytes L-02. The proliferation of hepatoma carcinoma SMMC-7721 cells and normal hepatocytes L-02 infected with the CASF/Ad complex was investigated. The viability of SMMC-7721 cells in the Ad-infected group was evidently lower than that of cells in the DMEM group after cultivation for 1, 3, 5 and 7 days. Furthermore, the viability of SMMC-7721 cells infected with the CASF/Ad complex and cultured for 1, 3, 5 and 7 days was significantly lower than that of cells infected with the naked Ad and cells cultured in DMEM. These results indicated that the ING4 and IL-24 genes expressed in Ad and CASF/Ad effectively inhibited the growth of hepatoma carcinoma SMMC-7721 cells. The CASF/Ad complex had higher infection efficiency than the naked Ad in SMMC-7721 cells, causing increased expression of ING4 and secretion of IL-24; thus, the CASF/Ad complex had enhanced growth inhibition in hepatoma carcinoma SMMC-7721 cells. The viability of L-02 cells infected with the CASF/Ad complex was not obviously different from that of cells infected with the naked Ad and cells cultured in DMEM, suggesting that the exogenous expression of ING4 and IL-24 caused no obvious toxic effects in normal hepatocytes. Coating Ad with CASF helps to increase the efficiency of vectors for gene therapy and enable the dose of adenovirus to be reduced and the efficiency to be maintained, possibly reducing the potential side effects of high doses of adenovirus.

Conclusions

An RGD-modified Ad vector coexpressing ING4 and IL-24 genes was constructed, and ASF modified with low-molecular-weight PEI was used to coat the vector by electrostatic interactions to form the CASF/Ad complex. Compared to the naked Ad with a particle diameter of approximately 81.03 nm and a zeta potential of −9.53 mV, the diameter of the CASF/Ad complex increased from 128.85 to 176.75 nm, and the zeta potential increased from −8.63 to −1.70 mV. It was found that the infection efficiency of both hepatoma carcinoma SMMC-7721 cells and hepatic L-02 cells infected with the CASF/Ad complex was significantly enhanced compared to that of cells infected with the naked Ad. The target gene ING4 in the CASF/Ad complex was efficiently expressed in SMMC-7721 cells, and the target gene IL-24 was effectively secreted from SMMC-7721 cells, inducing the apoptosis of hepatoma SMMC-7721 cells but showing no obvious toxicity in normal hepatic L-02 cells. The CASF/Ad complex used for gene vector might reduce the dose of adenovirus but still have high infection efficiency and can effectively promote tumor cell apoptosis, thus is possible to reduce potential side effects of high doses of adenovirus. This work provides a new gene therapy system for human hepatoma and might have potential use for the clinical treatment of human liver cancer.

Acknowledgments

The authors gratefully acknowledge Professor Weihua Sheng from College of Medicine in Soochow University for technical assistance.

Funding

This work has been funded by the National Key R&D Program of China (project 2017YFC113600, 2017YFC113602).

Disclosure

All authors report no conflicts of interest in this work.

References

1. Xia D, Feng LB, Wu XL, Xia GD, Xu L. Microencapsulation of recombinant adenovirus within poly-DL-lactide-poly (ethylene glycol) microspheres for enhanced gene transfection efficiency and inhibitory effects on hepatocellular carcinoma cells *in vitro*. *Mol Med Rep*. 2015;12:2336–2342.
2. Wang H, Guo R, Du ZH, et al. Epigenetic targeting of *Granulin* in hepatoma cells by synthetic CRISPR dCas9 Epi-suppressors. *Mol Ther-Nucl Acids*. 2018;11:23–33. doi:10.1016/j.omtn.2018.01.002
3. Bakhtiar A, Sayyad M, Rosli R, Maruyama A, Chowdhury EH. Intracellular delivery of potential therapeutic genes: prospects in cancer gene therapy. *Curr Gene Ther*. 2014;14:247–257.
4. Shi S, Zhu XC, Guo QF, et al. Self-assembled mPEG-PCL-g-PEI micelles for simultaneous codelivery of chemotherapeutic drugs and DNA: synthesis and characterization *in vitro*. *Int J Nanomed*. 2012; 7:1749–1759.
5. Zhao YD, Li ZY, Sheng WH, Miao JC, Yang JC. Adenovirus-mediated ING4/IL-24 double tumor suppressor gene co-transfer enhances antitumor activity in human breast cancer cells. *Oncol Rep*. 2012;28:1315–1324. doi:10.3892/or.2012.1930
6. Chen YS, Fu R, Xu MD, Huang YF, Sun GX, Xu LC. N-methyl-N-nitro-N-nitrosoguanidine-mediated ING4 downregulation contributed to the angiogenesis of transformed human gastric epithelial cells. *Life Sci*. 2018;199:179–187. doi:10.1016/j.lfs.2018.02.034
7. Caudell EG, Mumm JB, Poindexter N, et al. The protein product of the tumor suppressor gene, melanoma differentiation-associated gene 7, exhibits immunostimulatory activity and is designated IL-24. *J Immunol*. 2002;168:6041–6046. doi:10.4049/jimmunol.168.12.6041
8. Jiang G, Zhang K, Jiang AJ, et al. A conditionally replicating adenovirus carrying interleukin-24 sensitizes melanoma cells to radiotherapy via apoptosis. *Mol Oncol*. 2012;6:383–391. doi:10.1016/j.molonc.2012.05.001

9. Yang J, Yang J, Wei YH, et al. Modification of IL-24 by tumor penetrating peptide iRGD enhanced its antitumor efficacy against non-small cell lung cancer. *Int Immunopharmacol*. 2019;70:125–134. doi:10.1016/j.intimp.2019.02.027
10. Xie YF, Lv HT, Sheng WH, Miao JC, Xiang J, Yang JC. Synergistic tumor suppression by adenovirus-mediated inhibitor of growth 4 and interleukin-24 gene cotransfer in hepatocarcinoma cells. *Cancer Biother Radio*. 2011;26:681–695.
11. Vousden KH, Prives C. Blinded by the light: the growing complexity of p53. *Cell*. 2009;137:413.
12. Dewangan J, Srivastava S, Mishra S, Divakar A, Kumar S, Rath SK. Salinomycin inhibits breast cancer progression via targeting HIF-1α/VEGF mediated tumor angiogenesis *in vitro* and *in vivo*. *Biochem Pharmacol*. 2019;164:326–335. doi:10.1016/j.bcp.2019.04.026
13. Brat DJ, Bellail AC, Van Meir EG. The role of interleukin-8 and its receptors in gliomagenesis and tumoral angiogenesis. *Neuro Oncol*. 2005;7:122–133. doi:10.1215/S1152851704001061
14. Kim PH, Kim TI, Yockman JW, Kim SW, Yun CO. The effect of surface modification of adenovirus with an arginine-grafted bioreducible polymer on transduction efficiency and immunogenicity in cancer gene therapy. *Biomaterials*. 2010;31:1865–1874. doi:10.1016/j.biomaterials.2009.11.043
15. Fan GR, Fan MM, Wang Q, et al. Bio-inspired polymer envelopes around adenoviral vectors to reduce immunogenicity and improve *in vivo* kinetics. *Acta Biomater*. 2016;30:94–105. doi:10.1016/j.actbio.2015.11.005
16. Verma IM, Somia N. Gene therapy-promises, problems and prospects. *Nature*. 1997;389:239–242. doi:10.1038/38410
17. Bossche JVD, Jamal WTA, Yilmazer A, Bizzarri E, Tian B, Kostarelos K. Intracellular trafficking and gene expression of pH-sensitive, artificially enveloped adenoviruses *in vitro* and *in vivo*. *Biomaterials*. 2011;32:3085–3093. doi:10.1016/j.biomaterials.2010.12.043
18. Doronin K, Shashkova EV, May SM, Hofherr SE, Barry MA. Chemical modification with high molecular weight polyethylene glycol reduces transduction of hepatocytes and increases efficacy of intravenously delivered oncolytic adenovirus. *Hum Gene Ther*. 2009;20:975–988. doi:10.1089/hum.2009.028
19. Zeng Q, Han JF, Zhao D, Gong T, Zhang ZR, Sun X. Protection of adenovirus from neutralizing antibody by cationic PEG derivative ionically linked to adenovirus. *Int J Nanomed*. 2012;7:985–997.
20. Kim PH, Sohn JH, Choi JW, et al. Active targeting and safety profile of PEG-modified adenovirus conjugated with herceptin. *Biomaterials*. 2011;32:2314–2326. doi:10.1016/j.biomaterials.2010.10.031
21. Kim PH, Kim J, Kim TI, et al. Bioreducible polymer-conjugated oncolytic adenovirus for hepatoma-specific therapy via systemic administration. *Biomaterials*. 2011;32:9328–9342. doi:10.1016/j.biomaterials.2011.08.066
22. Zhao NX, Bagaria HG, Wong MS, Zu YL. A nanocomplex that is both tumor cell-selective and cancer gene-specific for anaplastic large cell lymphoma. *J Nanobiotechnol*. 2011;9:1–12. doi:10.1186/1477-3155-9-2
23. Park TG, Jeong JH, Kim SW. Current status of polymeric gene delivery systems. *Adv Drug Deliver Rev*. 2006;58:467–486.
24. Zou SZ, Wang XR, Fan SN, Zhang JM, Shao HL, Zhang YP. Fabrication and characterization of regenerated *Antheraea pernyi* silk fibroin scaffolds for Schwann cell culturing. *Eur Polym J*. 2019;117:123–133.
25. Zhao CX, Wu XF, Zhang Q, Yan SQ, Li MZ. Enzymatic degradation of *Antheraea pernyi* silk fibroin 3D scaffolds and fibers. *Int J Biol Macromol*. 2011;48:249–255. doi:10.1016/j.ijbiomac.2010.11.004
26. Fang Q, Chen DL, Yang ZM, Li M. *In vitro* and *in vivo* research on using *Antheraea pernyi* silk fibroin as tissue engineering tendon scaffolds. *Mat Sci Eng C*. 2009;29:1527–1534.
27. Patra C, Talukdar S, Novoyatleva T, et al. Silk protein fibroin from *Antheraea mylitta* for cardiac tissue engineering. *Biomaterials*. 2012;33:2673–2680. doi:10.1016/j.biomaterials.2011.12.036
28. Rocha LA, Learmonth DA, Sousa RA, Salgado AJ. αvβ3 and α5β1 integrin-specific ligands: from tumor angiogenesis inhibitors to vascularization promoters in regenerative medicine? *Biotechnol Adv*. 2018;36:208–227.
29. Asampille G, Verma BK, Swain M, et al. An ultra-stable redox-controlled self-assembling polypeptide nanotube for targeted imaging and therapy in cancer. *J Nanobiotechnol*. 2018;16:1–14. doi:10.1186/s12951-018-0427-1
30. Wang J, Zhang SS, Xing TL, et al. Ion-induced fabrication of silk fibroin nanoparticles from Chinese oak tasar *Antheraea pernyi*. *Int J Biol Macromol*. 2015;79:316–325. doi:10.1016/j.ijbiomac.2015.04.052
31. Yu YN, Hu YP, Li XF, et al. Spermine-modified *Antheraea pernyi* silk fibroin as a gene delivery carrier. *Int J Nanomed*. 2016;11:1013–1023.
32. Ping Y, Hu QD, Tang GP, Li J. FGFR-targeted gene delivery mediated by supramolecular assembly between β-cyclodextrin-crosslinked PEI and redox-sensitive PEG. *Biomaterials*. 2013;34:6482–6494. doi:10.1016/j.biomaterials.2013.03.071
33. Nurhasni H, Cao JF, Choi M, et al. Nitric oxide-releasing poly (lactic-co-glycolic acid)-polyethylenimine nanoparticles for prolonged nitric oxide release, antibacterial efficacy, and *in vivo* wound healing activity. *Inter J Nanomed*. 2015;10:3065–3080.
34. Zhang B, Zhang YY, Yu DM. Lung cancer gene therapy: transferrin and hyaluronic acid dual ligand-decorated novel lipid carriers for targeted gene delivery. *Oncol Rep*. 2017;37:937–944. doi:10.3892/or.2016.5298
35. Tan S, Wang GX. Lung cancer targeted therapy: folate and transferrin dual targeted, glutathione responsive nanocarriers for the delivery of cisplatin. *Biomed Pharmacother*. 2018;102:55–63. doi:10.1016/j.biopha.2018.03.046
36. Jin GW, Koo H, Nam K, et al. PAMAM dendrimer with a 1,2-diaminoethane surface facilitates endosomal escape for enhanced pDNA delivery. *Polymer*. 2011;52:339–346.
37. Han ZL, Zhou CY, Sun BC, Yan QH, Zhang JH. Experimental studies on the inhibition of adenovirus-ING4-OSM therapy on nasopharyngeal carcinoma proliferation *in vitro* and *in vivo*. *Cell Biochem Biophys*. 2014;70:1573–1578.
38. Oikawa K, Mizusaki A, Takanashi M, et al. PRG4 expression in myxoid liposarcoma maintains tumor cell growth through suppression of an antitumor cytokine IL-24. *Biochem Bioph Res Commun*. 2017;485:209–214. doi:10.1016/j.bbrc.2017.02.055
39. Hidaka C, Milano E, Leopold PL, et al. CAR-dependent and CAR-independent pathways of adenovirus vector–mediated gene transfer and expression in human fibroblasts. *J Clin Invest*. 1999;103:579–587. doi:10.1172/JCI5309
40. Moon CY, Choi JW, Kasala D, Jung SJ, Kim SW, Yun CO. Dual tumor targeting with pH-sensitive and bioreducible polymer-complexed oncolytic adenovirus. *Biomaterials*. 2015;41:53–68. doi:10.1016/j.biomaterials.2014.11.021
41. Maryam Y, Saeideh NR, Fereshteh H, et al. Physical characterization and uptake of iron oxide nanoparticles of different prostate cancer cells. *J Magn Magn Mater*. 2019;473:205–214. doi:10.1016/j.jmmm.2018.10.062
42. Luo J, Li CX, Chen JL, Wang G, Gao R, Gu ZW. An efficient method for *in vitro* gene delivery via regulation of cellular endocytosis pathway. *Int J Nanomed*. 2015;10:1667–1678.
43. Matsumura Y, Maeda H. A new concept for macromolecular therapeutics in cancer chemotherapy: mechanism of tumoritropic accumulation of proteins and the antitumor agent smancs. *Cancer Res*. 1986;46:6387–6392.
44. Salatin S, Dizaj SM, Khosroushahi AY. Effect of the surface modification, size, and shape on cellular uptake of nanoparticles. *Cell Biol Int*. 2015;39:881–890. doi:10.1002/cbin.10459.

45. Maeda M, Kida S, Hojo K, et al. Design and synthesis of a peptide-PEG transporter tool for carrying adenovirus vector into cells. *Bioorg Med Chem Lett*. 2005;15:621–624. doi:10.1016/j.bmcl.2004.11.055
46. Eto Y, Gao JQ, Sekiguchi F, et al. PEGylated adenovirus vectors containing RGD peptides on the tip of PEG show high transduction efficiency and antibody evasion ability. *J Gene Med*. 2005;7:604–612. doi:10.1002/jgm.699
47. Li P, Shi YW, Li BX, et al. Photo-thermal effect enhances the efficiency of radiotherapy using Arg-Gly-Asp peptides-conjugated gold nanorods that target αvβ3 in melanoma cancer cells. *J Nanobiotechnol*. 2015;13:1–8. doi:10.1186/s12951-015-0113-5
48. Cun YP, Zhang QH, Xiong CJ, et al. Combined use of adenoviral vector Ad5/F35-mediated APE1 siRNA enhances the therapeutic efficacy of adenoviral-mediated p53 gene transfer in hepatoma cells *in vitro* and *in vivo*. *Oncol Rep*. 2013;29:2197–2204. doi:10.3892/or.2013.2384
49. Huang ZG, Lv FM, Wang J, et al. RGD-modified PEGylated paclitaxel nanocrystals with enhanced stability and tumor-targeting capability. *Int J Pharm*. 2019;556:217–225. doi:10.1016/j.ijpharm.2018.12.023